

University of Massachusetts Amherst

From the Selected Works of William MacKnight

1979

Modeling of Tensile Properties of Polymer Blends: PPO/Poly(styrene-co-p chlorostyrene)

William MacKnight, *University of Massachusetts Amherst*
J. R. Fried



Available at: https://works.bepress.com/william_macknight/239/

Modeling of tensile properties of polymer blends: PPO/poly(styrene-co-*p*-chlorostyrene)

J. R. Fried

Department of Chemical and Nuclear Engineering and the Polymer Research Center, University of Cincinnati, Cincinnati, Ohio 45221

W. J. MacKnight and F. E. Karasz

Polymer Science and Engineering Department and the Materials Research Laboratory, University of Massachusetts, Amherst, Massachusetts 01003

Young's modulus, yield (break) strength, and elongation to yield (break) have been measured for blends of poly(2,6-dimethyl-1,4-phenylene oxide) (PPO) with polystyrene (PS), poly(*p*-chlorostyrene) (PpClS), and random copolymers of styrene and *p*-chlorostyrene (pClS). The significant difference between blend compositions is the compatibility of PPO with each styrene polymer. Blends of PPO with PS or copolymers with 67.1 mole% or less pClS are compatible (i.e., one T_g) and show small synergistic maxima in modulus, strength, and elongation as a function of PPO composition. These maxima correspond to observed maxima in packing density as a result of specific interactions contributing to blend compatibility. A rule of mixtures for one-phase systems with an adjustable compatibility parameter gives adequate fit to the observed composition dependence of the modulus. In a narrow composition range between 67.8 and 68.6 mole% pClS, copolymers exhibit partial miscibility with PPO. Two mixed composition phases are present. Moduli of these transitional blends follow the same form of synergistic dependence on blend composition as do the compatible blends but strength and elongation exhibit a sigmoidal relation to blend PPO content. At about 20% PPO, strength (and elongation) reaches a minimum as predicted by a simple composite model for a dispersed phase with good adhesion to the matrix. A maximum is reached at ~80% PPO at which composition blend test specimens yield prior to failure. Blends of PPO with PpClS and with copolymers of > 68.6 mole% pClS exhibit a broader minimum in strength (and elongation) but a similar maximum at 80% PPO. Unlike the compatible and transitional blends, moduli follow a nonsynergistic composition dependence adequately represented by the series model for two-phase systems.

PACS numbers: 46.30.Cn

I. INTRODUCTION

The mechanical properties of filled polymer composites have been widely studied and theories modeling their behavior have been successful in achieving at least a practical understanding of how filler shape, size, concentration, modulus, and interfacial adhesion relate to the properties of the matrix polymer in determining the overall mechanical response of the composite. Much less attention has been directed toward understanding how the mechanical properties of polyblends, in which both components are polymeric, are related to the properties of the individual components. Qualitatively, it is recognized that blends of two polymers that are not mutually miscible, i.e., are incompatible, form separate phases that are generally less well defined in size and shape than in controlled composite formulations. Films, fibers, and molded parts of such incompatible blends are opaque and have low strength and toughness as a result of poor adhesion between phases.¹ At the other extreme, compatible polyblends in which the component polymers do not phase separate but instead form a microscopically homogeneous single phase have high strength and form clear films. In certain cases, both modulus² and tensile strength³ have been reported to be greater at particular blend compositions than the corresponding properties of either polymer in the unblended state. Such synergism in modulus and strength is apparently achieved at the expense of impact strength as ductile polymers will undergo embrittlement as a result of

blending with another compatible polymer in apparent analogy to polymers antiplasticized with low molecular weight additives.^{3,4}

In this paper, an attempt is made to relate the mechanical (tensile) properties of a family of related polyblends to the state of compatibility of the blend. The prototype compatible blend studied is that of poly(2,6-dimethyl-1,4-phenylene oxide) (PPO) and polystyrene (PS). Evidence for the compatibility of PPO and PS is substantial and is reviewed elsewhere.⁵ Films molded from blends of PPO and PS are optically clear and exhibit a single composition-dependent glass transition temperature (T_g).

By contrast, PPO is *not* compatible with chlorinated PS, either poly(*p*-chlorostyrene) (PpClS) or poly(*o*-chlorostyrene) (PoClS). Blends of PPO with either PpClS or PoClS form opaque films and exhibit two glass transitions identical in temperature and dispersion width to those of the corresponding unblended polymers. The independence of phase T_g on blend composition (weight fraction PPO) for PpClS/PPO blends is illustrated in Fig. 1. In addition, fracture replicas of PpClS/PPO blends indicate macroscopic phase separation of the component polymers into large irregular-shaped domains.⁷

Blend compatibility can be varied systematically by blending PPO with random copolymers of styrene and *p*-chlorostyrene (pClS).^{6,8} Copolymers with low pClS content (<67.1 mole% pClS) are compatible with PPO as evidenced

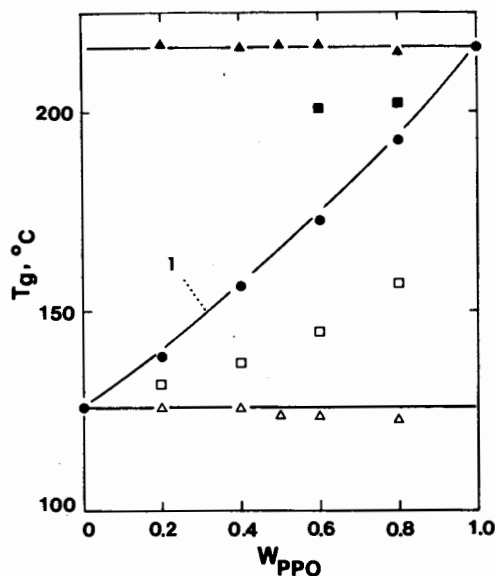


FIG. 1. Blend glass transition temperature (T_g) as a function of weight fraction PPO (W_{PPO}): (●) copolymer B/PPO; (■) copolymer D/PPO, high-temperature transition; (□) copolymer D/PPO, low-temperature transition; (▲) PpCIS/PPO, high-temperature transition; (△) PpCIS/PPO, low-temperature transition (each point dropped 7 °C on the ordinate for purpose of comparison with the lower T_g copolymers). Curve 1 was drawn from values of T_g 's calculated by means of the Couchman equation [Eq. (1)] for the compatible copolymer B/PPO blends.

by film clarity and by a single T_g at each blend composition. Recently, Couchman⁹ has shown that the T_g of these compatible blends follows a composition dependence given as

$$\ln\left(\frac{T_g}{T_{g1}}\right) = \left[W_2 \Delta C_{p2} \ln\left(\frac{T_{g2}}{T_{g1}}\right) \right] \times (W_1 \Delta C_{p1} + W_2 \Delta C_{p2})^{-1}, \quad (1)$$

where W and ΔC_p are weight fraction and change in heat capacity at T_g , respectively, for components 1 (copolymer) and 2 (PPO) as indicated. The form of this dependence is illustrated for blends of a copolymer with 58.5 mole% pCIS (copolymer B) and PPO in Fig. 1. As PPO is blended with copolymers of increasing pCIS content, the dispersion width of the single glass transition of the compatible copolymer/PPO blends increases. This broadening of the transition width has been directly related to an increase in localized concentration fluctuations in the blend, i.e., increasing blend heterogeneity.¹⁰

TABLE II. Properties of blend polymers

Polymer	mole% pCIS	T_g (°C) ^a	$\bar{M}_n \times 10^{-3}$	$\bar{M}_w \times 10^{-3}$	E (GPa)	σ (MPa)	ϵ (%)
Copolymer B	58.5	125	95	208	3.40	49 ^b	1.2 ^b
Copolymer D	67.8	126	100	192	3.15	45 ^b	1.1 ^b
PpCIS	100	132	128	217	3.49	46 ^b	1.1 ^b
PPO	...	216	17	35	2.66	71 ^c	2.7 ^c

^aDSC; 20 °/min.

^bBreak.

TABLE I. Three compatibility categories based on the pCIS composition of the copolymer

mole% pCIS	Classification	Blend Morphology
0-67.1	Compatible	Homogeneous
67.8-68.6	Transitional	Small mixed composition domains; large interfacial regions
75.4-100	Incompatible	Large homogeneous domains; small interfacial regions

Blends of PPO and copolymers in the narrow composition range between 67.8 and 68.6 mole% pCIS exhibit phase separation as evidenced by the detection of two glass transitions; however, these transitions are not as well defined as those of the incompatible PpCIS/PPO, PoCIS/PPO, and higher pCIS copolymer/PPO blends. They are considerably broadened, diminished in intensity (ΔC_p), and shifted in temperature when compared to the corresponding unblended components. This intermediate character of these "transitional" blends is illustrated by the T_g -composition dependence of copolymer D (67.8 mole% pCIS)/PPO blends in Fig. 1 where T_g data points fall between the curve given by Eq. (1) for the compatible blends and the horizontal lines representing the composition independent T_g 's of the two-phase incompatible blends.

The shifting of component T_g 's suggests that the above marginally compatible blends are composed of mixed-composition domains, a PPO-rich (high T_g) phase and a copolymer-rich (low T_g) phase. As has been observed directly for other incompatible blends,¹¹ it is probable that the domains themselves are separated by diffuse interfacial regions. The presence of large diffuse interfacial regions would explain the observed reduction of blend ΔC_p .⁶ Films of these blends are either clear or hazy depending on the PPO composition of the blend.

In summary of the above results, PPO/poly(styrene-*co*-*p*-chlorostyrene) blends may be divided into three compatibility categories depending upon the pCIS composition of the copolymer as given in Table I. The mechanical properties of blends representing these three blend categories have been measured as a function of blend composition (volume fraction PPO) and are reviewed below with respect to current theories of composite behavior.

II. EXPERIMENTAL

Methods of copolymer and blend preparation have been detailed elsewhere.⁶ The physical and mechanical

^cYield.

properties of those polymers whose blend mechanical properties reported here are summarized for convenience in Table II.

Miniature dumbbell-shaped specimens of each polymer and blend were molded from pieces of compression molded films by means of a Mini-Max Injection Molder (Custom Scientific Instruments) whose operation and mixing characteristics have been reviewed by Maxwell.¹² The Gauge length of the molded dumbbells was 8.9 mm at a cross-sectional diameter of 0.157 cm.

Cup and mold temperatures were raised by increments of 20 °C for each blend increment of 20 wt% PPO from a lower limit of 250 °C for PS, the copolymers, PpCIS, and PoCIS to a high of 340 °C for unblended PPO. After injection, molds were removed, placed on a large metal plate, and allowed to slowly cool to ambient temperature (23 °C). In this manner, blends were cooled at rates comparable to the controlled rates used in previous DSC studies of these blends.⁶ Studies of *n*-hexane induced crazing of PS/PPO molded specimens using the above techniques indicated no preferential orientation of crazes, whereas rapidly quenched samples exhibited craze orientation parallel to the injection (axial) direction.^{2b}

Measurements of tensile properties were made at room temperature by means of a Tensilon UTM-II mechanical tester (Toyo Baldwin Co., Ltd.) at a constant crosshead speed of 0.2 mm min⁻¹ corresponding to a nominal strain rate of 3.75×10^{-4} sec⁻¹. Young's modulus (*E*) was arbitrarily defined as the secant modulus at 0.6% elongation and is expressed in SI units of GPa (GPa = 10¹⁰ dyn/cm²). Ultimate strength (σ_u) and elongation (ϵ_u) were defined as the stress and engineering strain, respectively, at break. Yield strength (σ_y) and elongation (ϵ_y) were taken as the stress and engineering strain at the maximum in the stress-strain curve. The values of σ and ϵ are expressed in MPa (MPa = 10⁷ dyn/cm²) and %, respectively. Measured ϵ was corrected for finite sample gauge length and instrumental compliance

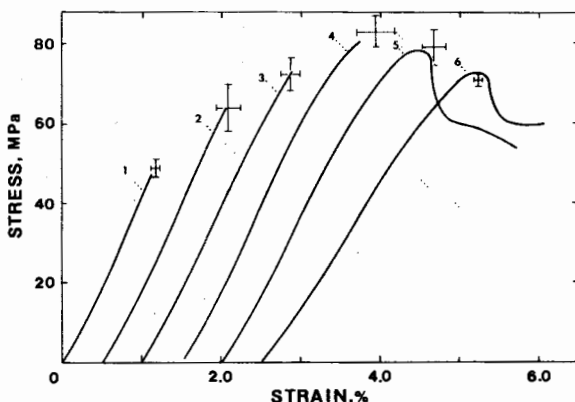


FIG. 2. Representative stress-strain curves of the compatible copolymer B/PPO blends. Curve 1, copolymer B; curve 2, 20% PPO; curve 3, 40% PPO; curve 4, 60% PPO; curve 5, 80% PPO; curve 6, 100% PPO. Error bars indicate 95% confidence intervals for both stress and strain at break (or yield) for sample populations. Curves 2-6 have been sequentially shifted 0.5% in strain along the abscissa for the purpose of comparison.

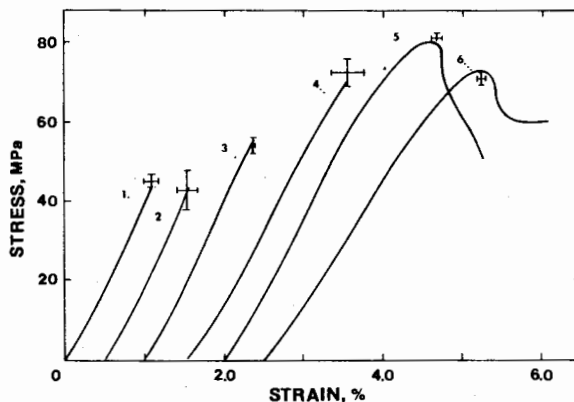


FIG. 3. Stress-strain curves of the transitional copolymer D/PPO blends. Identification is the same as in Fig. 2 except that curve 1 represents unblended copolymer D (0% PPO).

as detailed elsewhere.¹³ Values for *E*, σ and ϵ were reported as population mean values for 4-15 samples according to standard small sampling techniques; error bars indicate 95% confidence limits.

III. RESULTS

Representative stress-strain curves for the compatible copolymer B/PPO, transitional copolymer D/PPO, and incompatible PpCIS/PPO blends are illustrated in Figs. 2-4. Qualitatively, one of the more notable results illustrated by these series of curves in an apparent embrittlement at high PPO blend compositions as the mode of failure changes from one of predominantly brittle fracture at below 80% PPO to ductile or yielding behavior at and above 80% PPO. Embrittlement of PPO by PS has been reported to accompany a suppression of the low-temperature β relaxation of PPO in analogy to the observed embrittlement of ductile polymers antiplasticized by low molecular weight additives.^{3,4} Wellinghoff and Baer³ have shown that this observed embrittlement of PPO by PS in these compatible blends corresponds to a change in the process of deformation from one of diffuse shear banding (type-II glass) to one of extensive craze initiation and growth (type-I glass). The deformation microstructure of the copolymer/PPO blends, although not reviewed in the present study, are under investigation and will await future publication.

As Fig. 2 illustrates, the stress at break (or yield) of the compatible copolymer B blends rises to a maximum at between 60 and 80% PPO. This apparent enhancement in strength has been observed in the case of polymers antiplasticized by low molecular weight additives¹⁴ and suggests that the compatible copolymers act as polymeric antiplasticizers for PPO. This analogy to antiplasticization has been applied to other compatible polymer blends.^{15,16} Similar synergistic dependence of tensile strength on blend composition for PS/PPO blends has been reported.^{13,17} In a study of tensile behavior over several decades of strain rate, Yee³ has shown that actually two maxima in strength may be evident in the case of PS/PPO blends: one at below 20% PPO and the

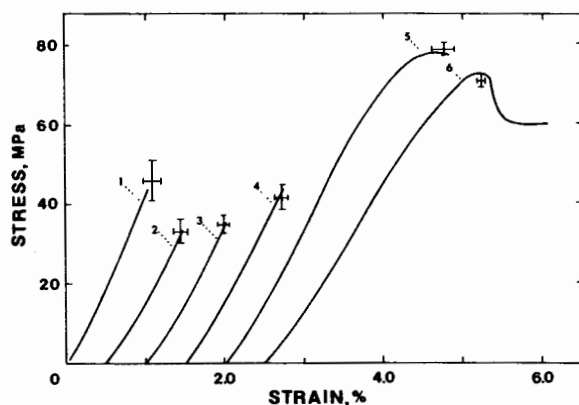


FIG. 4. Stress-strain curves of the incompatible PpClS/PPO blends. Identification is the same as in Fig. 2 except that curve 1 represents unblended PpClS (0% PPO).

other at above 75% PPO. The low PPO maximum was found to decrease in intensity with decreasing strain rate ($\dot{\epsilon}$). A second low % PPO maximum may occur for the compatible PS/PPO and copolymer B/PPO blends reported here, but Yee's results suggest that for the particular blend compositions (none less than 20% PPO) and relatively large strain rates chosen here, this maximum may escape detection.

Stress-strain curves for the transitional copolymer D/PPO and incompatible PpClS/PPO blends given in Figs. 3 and 4, respectively, again indicate embrittlement at 60–80% PPO. Unlike unblended PPO and the high PPO content compatible blends that yield and cold draw, the high PPO content two-phase blends do not appear to initiate a stable neck region and failure occurs shortly after the yield point.

In comparison to the monotonic increase in strength exhibited by the compatible copolymer B blends with increasing PPO content, the transitional copolymer D and incompatible PpClS blends (Figs. 3 and 4) reach a minimum in break strength at 20–40% PPO. For example, the break strength of 80% PpClS/20% PPO is approximately 28% lower than the break strength of PpClS alone. These observations of break strength reduction along with the results of blend modulus behavior are analyzed below with respect to current theories of polymer composite behavior.

IV. DISCUSSION

A. Modulus

The maximum modulus of a composite is given by the rule of mixtures.¹⁸

$$E = V_1 E_1 + V_2 E_2, \quad (2)$$

where V represents the volume fraction of component 1 or 2. The lowest value of modulus is given by the series model.¹⁹

$$1/E = V_1/E_1 + V_2/E_2. \quad (3)$$

Values predicted by other equations such as those proposed by Kerner, Nielsen, Van der Poel, Grezczuk, Sato and Furukawa, Eilers-Van Dijk, and others fall between the bounds set by Eqs. (2) and (3).

Until recently, little attention has been given to predicting the modulus of polyblends. The first obvious distinction between polyblends and composites is that whereas the ratio of filler modulus to polymer modulus in composites is typically greater than 20,²⁰ the ratio of moduli for polyblends is very nearly equal to unity. For this reason of component modulus equivalency in polyblends, the form of the dependence of polyblend moduli on blend composition may be difficult to model in any meaningful manner with the limitation of typical scatter of experimental data.

Recently, Kleiner *et al.*² have shown that the moduli of the compatible PS/PPO blends fall outside the upper bounds given by Eq. (2). Instead of the classical composite results, the blend moduli are reported to follow a composition dependency given by the general equation cited by Nielsen²¹ for one-phase binary mixtures in the specific form given by Kleiner

$$E = V_1 E_1 + V_2 E_2 + \beta_{12} E_1 E_2. \quad (4)$$

The empirical interaction term, β_{12} , in Eq. (4) is given as

$$\beta_{12} = 4 E_{12} - 2 E_1 - 2 E_2, \quad (5)$$

where E_{12} represents the measured modulus of a 50/50 (PS/PPO) blend. As an interaction term, β_{12} may be a relative measure of blend compatibility. It was shown that β_{12} increased with decreasing molecular weight of the PS component, i.e., in the direction of increasing blend compatibility. Kleiner postulated that the origin of the synergism in modulus suggested by the form of Eq. (4) and demonstrated experimentally in the case of PS/PPO is the observed increase in packing density due to blending. Spectroscopic evidence for specific interactions between PPO and PS that may account for such densification has been given.²²

The calculated moduli of the compatible copolymer B/PPO blends are plotted against volume fraction PPO (V_{PPO}) in Fig. 5. The solid curve is drawn using Eq. (4) and

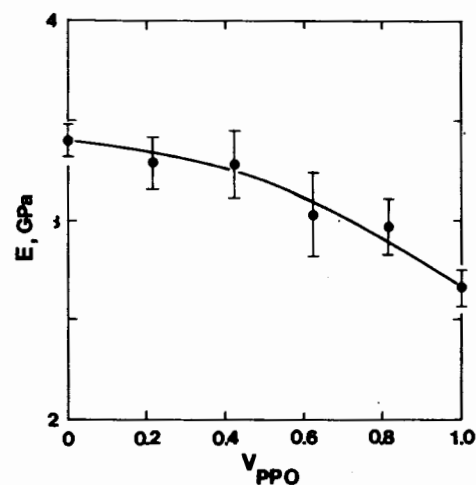


FIG. 5. Young's modulus (E) as a function of volume fraction PPO (V_{PPO}) for the compatible copolymer B/PPO blends. The curve was drawn by use of the modified rule of mixtures for composites [Eq. (4)].

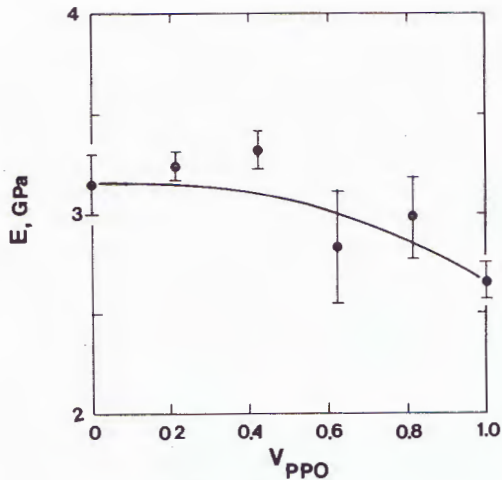


FIG. 6. Young's modulus versus volume fraction PPO for the transitional copolymer D/PPO blends. Curve, Eq. (4).

an empirical value of 0.66 for β_{12} as found by Kleiner to give best fit for the PS/PPO blends when PS is Monsanto HH 101 grade (similar molecular weight and molecular weight distribution to the copolymer). The good agreement between the experimental moduli and the empirical Kleiner curve as illustrated in Fig. 5 suggests an equivalent compatible state in the copolymer B/PPO blends as compared to the PS/PPO blends and as substantiated in prior publications by calorimetric⁶ and dielectric¹⁰ studies. Scanning electron micrographs of cold fractured tensile specimens of these compatible copolymer/PPO blends reveal no evidence of macrophase structure at $1000\times$.¹³

The transitional blends as defined in Sec. III also appear to follow Eq. (4) as illustrated by the data and the empirical curve in Fig. 6. It is noted that both the compatible and transitional blends exhibit packing densification⁶ supporting the explanation given by Kleiner for the modulus behavior.

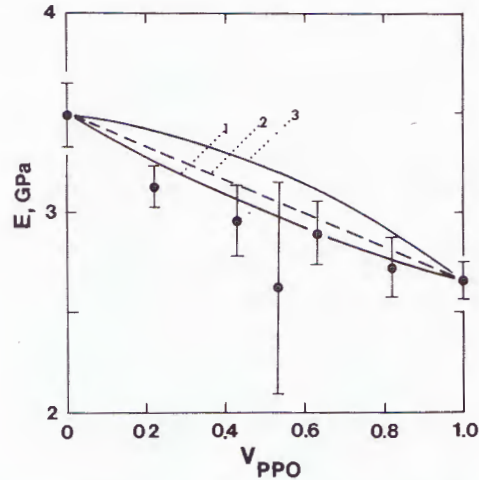


FIG. 7. Young's modulus versus volume fraction PPO for the incompatible PpCIS/PPO blends. Curve 1, the series model [Eq. (3)]; curve 2, rule of mixtures [Eq. (2)]; curve 3, modified rule of mixtures [Eq. (4)].

Finally, moduli of the incompatible PpCIS/PPO blends are plotted against blend composition in Fig. 7. As shown, experimental values are much lower on the ordinate than would be predicted for a compatible (and transitional) blend on the basis of Eq. (4) (upper curve in Fig. 7) but are well approximated by a composite series model given by Eq. (3) (lower curve). The moduli of PPO/glass bead composites are reported by Trachte and DiBenedetto²³ to follow the Kerner equation and by Wambach *et al.*²⁴ to follow the equation of Van der Poel. These may therefore be more appropriate choices in modeling the composite behavior of the PpCIS/PPO blends but considering the low moduli ratio of the PpCIS/PPO blends, $E_{\text{PpCIS}}/E_{\text{PPO}} = 1.3$, the difference between values of moduli predicted by use of either of these equations or use of the simpler Eq. (3) would be slight.

Tkacik^{7b} has shown by means of transmission electron micrographs of molded films of PpCIS/PPO blends frac-

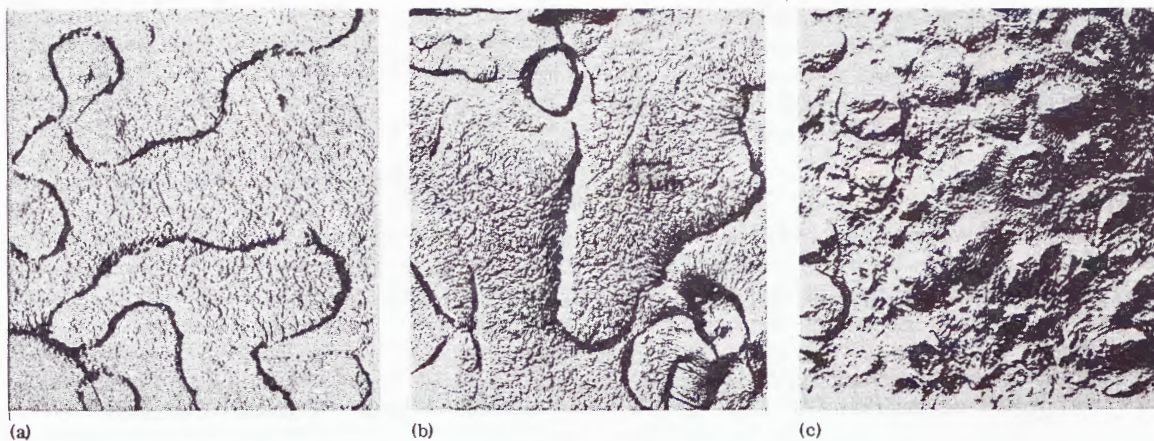


FIG. 8. Transmission electron micrographs of hot (170 °C) fractured molded films of PpCIS/PPO. Surface replicas prepared on carbon supports using gold-palladium shadowing. (a) 25% PPO; (b) 50% PPO; (c) 75% PPO. Reproduced with permission from Tkacik [Ref. 7(b)].

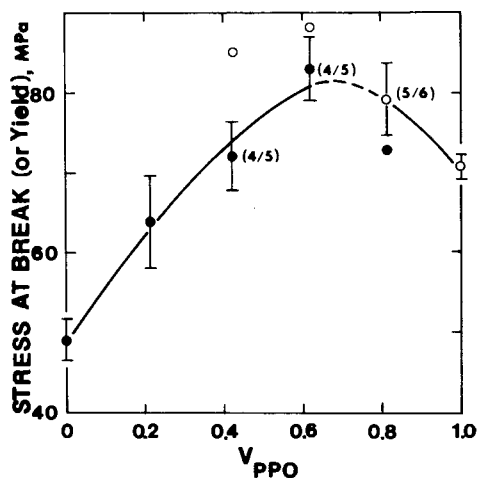


FIG. 9. Tensile stress at break (or yield) versus volume fraction PPO for the compatible copolymer B/PPO blends: (●), break strength; (○), yield stress. Error bars indicate 95% confidence limits. Values within parentheses indicate fraction of samples within test population that fail by predominant mode in the embrittlement region.

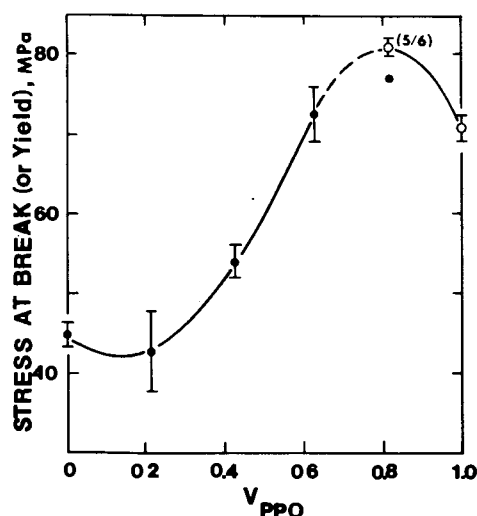


FIG. 10. Tensile stress at break (or yield) versus volume fraction PPO for the transitional copolymer D/PPO blends. Identification is the same as in Fig. 9.

tured at above the T_g of PpCIS that these blends exhibit macrophase separation ($> 10 \mu\text{m}$) as illustrated by the series of micrographs in Fig. 8. At blend compositions of 25 and 50% PPO, these blends are characterized by large irregular shaped domains of PPO polymer dispersed in a PpCIS matrix. Phase inversion resulting in a PpCIS dispersed phase and PPO matrix occurs at 75% PPO blend content. It is noted that the specific phase morphology of the injected molded tensile specimens used in the present study may differ from the compression molded film morphology. In the case of extruded samples of polymer blends displaying macrophase separation, Van Oene²⁵ indicates that the disperse phase may appear as either ribbons (stratification) or droplets independent of shear strain rate but dependent on the postextrusion thermal history. A study of the effect of morphology and phase inversion on the mechanical properties of the incompatible PPO blends is presently in progress.

In addition to the compositelike morphology of the PpCIS/PPO blends, these incompatible blends exhibit no blend densification in contrast to the compatible and transitional blends.⁶ Absence of blend densification would suggest no synergism in modulus in accordance with the Kleiner argument and in agreement with the experimental results.

B. Tensile strength

Strength at break (or yield) is plotted against volume fraction PPO (V_{PPO}) in Figs. 9–11 for the compatible, transitional, and incompatible blends whose moduli are plotted in Figs. 5–7. As previously reported for the prototype PS/PPO blends,^{3,13} and as qualitatively shown by the stress-strain curves in Fig. 2, the compatible copolymer B/PPO blends (Fig. 9) exhibit apparent synergism in tensile strength; i.e., the highest blend break strength is greater than the stress at break of the copolymer alone and correspondingly the highest yield stress of the blend is larger than the

measured yield stress of PPO in the unblended state. Embrittlement, or the transition from the brittle to ductile mode of failure, occurs at the same 60–80% PPO range in blend composition as observed in the PS/PPO blends.^{3,13} As indicated in Figs. 9–11, some tensile specimens break by either brittle or ductile failure at the same blend composition. The fraction of total specimens tested that fail in the predomi-

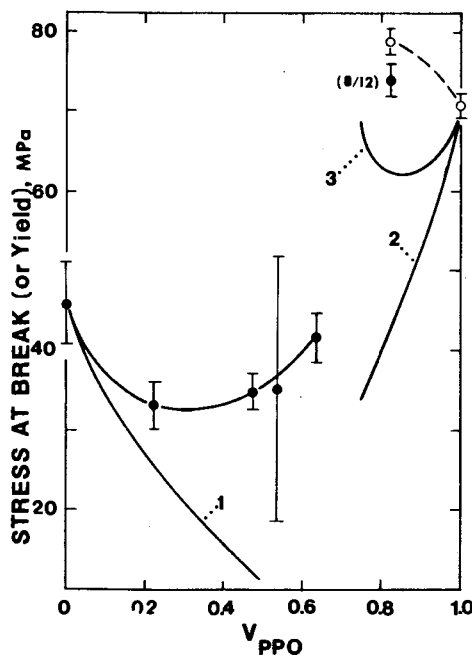


FIG. 11. Tensile stress at break (or yield) versus volume fraction PPO for the incompatible PpCIS/PPO blends. Identification is the same as in Fig. 9. Curve 1, the Schragger model for poor adhesion [Eq. (6), $r = 2.66$]; curve 2, data for untreated glass bead/PPO composites (Ref. 24); curve 3, silane treated glass bead/PPO composites (Ref. 24).

nant mode is indicated within the parentheses in each figure. In all cases, the yield stress is greater than the break stress. These observations may be explained in terms of the failure criteria proposed by Nicolais and DiBenedetto²⁶ for which brittle failure will occur if an individual sample defect grows to a critical defect size before the stress-strain curve reaches a maximum. Variations in defect size and defect size distribution within a tensile sample population result in a proportion of some samples failing in the brittle mode and some in the ductile mode within the embrittlement region.

That the compatible PPO blends appear to exhibit synergism in tensile strength can be interpreted in several ways. Extension of the rubber network theory²⁷ would suggest that an increase in strength could result from an increase in the number of network chains per unit volume formed by the entanglements. Increased entanglement density may occur as a result of specific interchain interactions such as those reported in the case of PS/PPO blends by Wellinghoff *et al.*²² However, recent rheological studies of PS/PPO blends indicate that the dependence of blend entanglement molecular weight (M_e) on blend composition falls between the linear rule of mixtures given by Eq. (2) if E is replaced by M_e and the series model in the similarly modified form of Eq. (3).²⁸ These results would suggest that in direct contrast to the experimentally found enhancement in tensile strength, the tensile strength of the blend should be at best a linear function of PPO content if the entanglement explanation is valid.

An alternate explanation for synergism in tensile strength may be taken from the same packing density argument proposed by Kleiner² to explain the observed synergism in modulus. Borrowing from the theory of the mechanics of crystal structure, Buchdahl²⁹ suggests that the (shear) strength of amorphous glassy polymers can be shown to be inversely proportional to the spacing between chain segments (i.e., packing density). In other words, the maximum in blend strength may be directly related to the maximum in blend density previously reported for these blends.⁶

Alternatively, it may be argued that the suppression of the β relaxation of PPO by PS as indicated by dynamic mechanical studies^{3,4} raises the stress level required to activate significant strain softening. The importance of the β relaxation in controlling stress-activated processes has been revealed in a study of several poly(vinyl chloride) polymer blends.^{15,16}

In contrast to the compatible PPO blends, the transitional blends exhibit a sigmoidal dependence of σ on V_{PPO} (Fig. 10). A minimum is reached between 10 and 20% PPO while at 60–80% PPO a maximum appears to exist at the same level and in the same composition range as found for the compatible blends. The embrittlement transition is again apparent at high V_{PPO} but more samples fail in the brittle mode at between 60 and 80% PPO than at corresponding blend compositions in the case of the compatible blends.

The incompatible blends of PpCIS/PPO exhibit a much broader minimum in σ (Fig. 11) but again σ appears to reach a synergistic level at 80% PPO. More samples fail in the brittle mode at corresponding compositions than do the

compatible and transitional blends in the embrittlement region. Additional data is required in the 80–100% PPO region to ascertain whether in fact a local minimum in σ may occur in the yield region as is clearly observed in the brittle zone or if in fact the high σ at 80% PPO is a true synergistic effect. Measurement of compressive strengths over a wider range of blend compositions is presently in progress and should provide a more conclusive picture.

If the modulus behavior suggests as previously illustrated that the incompatible PpCIS/PPO blends behave as composites, then the tensile strength of these blends may be expected to follow classical composite behavior as well. As discussed below, the dependence of σ on V_{PPO} as shown for PpCIS/PPO in Fig. 11 appears more complicated than expected for a simple composite with controlled dispersed phase composition, size, and aggregation as may be achieved for PPO/glass beads composites as an example.

In modeling filled polymer composites, Schragger³⁰ has recently proposed an equation useful for predicting the break strength in the case where the filler is not treated to improve adhesion. The form of the Schragger equation is given as

$$\sigma = \sigma_0 \exp(-rV), \quad (6)$$

where σ_0 is the strength of the matrix polymer, V is the volume fraction filler, and r is an interfacial parameter which is found to be 2.66 for many composites including PPO/glass beads.

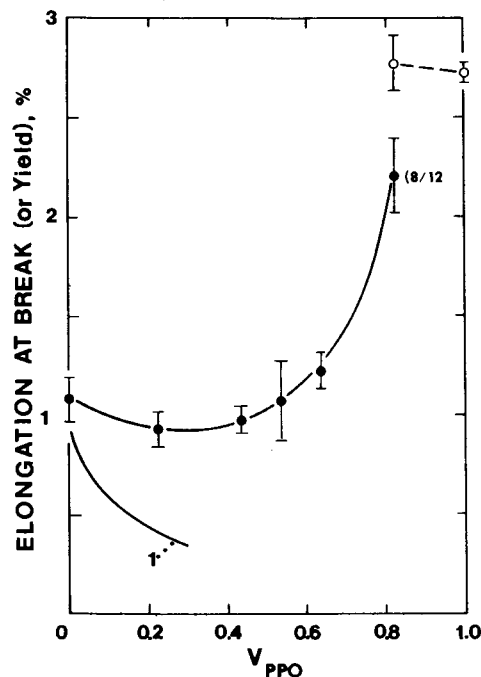


FIG. 12. Percent elongation at break (yield) for the incompatible PpCIS/PPO blends. (●), elongation at break; (○), elongation at yield. Values within parentheses indicate the fraction of samples failing in the principal mode in the embrittlement region. Error bars indicate 95% confidence intervals. Curve 1 was drawn from values calculated from the Nielsen model for perfect adhesion composites [Eq. (7)].

As illustrated in Fig. 11, the σ of the PpClS/PPO blends agree with values predicted by Eq. (6) only at low loadings, i.e., $V_{\text{PPO}} < 0.05$. At higher V_{PPO} , the observed blend σ is much larger than values predicted by Eq. (6). If one assumes that the interfacial adhesion between the PpClS and PPO phase is greater than could be expected in the case of a polymer matrix and an untreated inorganic filler for which Eq. (6) is valid, then the inadequacy of Eq. (6) to model the PpClS/PPO blend results is not surprising.

In the case of perfect adhesion as for example when silane coupling agents are used to bond the filler to the matrix, Nielsen³¹ has suggested that the elongation to break of the composite (ϵ) may be approximated by the following simple equation relating the elongation to break of the matrix (ϵ_0) and the volume fraction filler:

$$\epsilon \approx \epsilon_0(1 - V)^{1/3}. \quad (7)$$

Composite break strength is then calculated by substituting Eq. (7) and a composite model equation for modulus into a linear stress-strain relation ($\sigma = E\epsilon$). Qualitatively, the resulting expression predicts that σ should rapidly fall to a minimum at $\sim 10\%$ filler and then increase to values equal to or greater than σ_0 depending upon which expression for modulus is substituted into the Hookean relation.

Quantitatively, the Nielsen expression for elongation to break [Eq. (7)] has been reported to give good fit for some composites³² but underestimates ϵ in others such as the silane treated glass beads/epoxy system studied by Kenyon and Duffy.³³ In addition, Piggot and Leidner³⁴ have criticized the validity of the simple geometrical considerations upon which Eq. (7) is based. As shown in Fig. 12 for the composition range in which brittle failure is observed to occur in the PpClS/PPO blends, experimental values for break elongation consistently fall far above the curve calculated by use of Eq. (7). The usefulness of Eq. (7) in predicting ϵ (and therefore σ) in these incompatible polymer blends is inherently restricted by the basic assumption upon which Eq. (7) is derived—i.e., that the dispersed phase is infinitely rigid. In the case of glass filled composites, this assumption can be considered adequate but in the case of polyblends for which the ratio of the moduli of the dispersed phase and the matrix polymer is nearly unity (a ratio of 1.3 in the PpClS/PPO blends), only a qualitative representation of break elongation and therefore break strength can be expected. In consideration of these limitations, it is noted that the minimum in break strength that occurs at 15% PPO in the transitional copolymer D/PPO blends (Fig. 10) is in qualitative agreement with the Nielsen composite model for perfect adhesion between dispersed phase and matrix. By comparison, the minimum in break strength for the case of the incompatible PpClS/PPO blends (Fig. 11) is located at higher V_{PPO} and is deeper suggesting the probable importance of blend of compatibility in determining the strength of the interfacial adhesion and thereby the break strength of the polyblend composite.

Additional differences in the compositional dependence of the tensile strength between incompatible polymer blends and polymer composites are revealed by directly comparing tensile strengths of PpClS/PPO blends

($V_{\text{PPO}} \geq 0.8$) with those of PPO filled with glass beads (1–30 μm) as given by Wambach *et al.*²⁴ Values for E and σ_y of unfilled PPO (2.55 GPa and 76.5 MPa, respectively) agree within confidence limits with those given in Table II at the same nominal strain rate and at nearly equivalent temperatures. In the upper right-hand portion of Fig. 11, the experimental yield strength of these glass bead/PPO composites is plotted versus V_{PPO} ($= 1 - V_{\text{beads}}$) for the case in which the beads are untreated (curve 2) and the break strength when a silane coupling agent is used (curve 3). In the former case, the curve closely agrees with the model proposed by Schrage [Eq. (6)] for poor adhesion, while the latter curve (qualitatively) agrees with the Nielsen prediction for a minimum at 15% filler for the case of perfect adhesion (silane coupling) between the dispersed phase and matrix. In striking contrast are the corresponding values for stress at yield for PPO with 20% PpClS “filler.” Instead of the expected reduction in yield strength due to the presence of a filler, the blend strength is actually about 11% higher than σ_y of unfilled PPO and is comparable to the values found for the compatible and transitional blends at the same blend compositions.

In addition, there are differences in the shape of the stress-strain curves between those of the glass bead/PPO composites and the PpClS/PPO incompatible blends. In the case of glass bead/PPO³² and other glass bead filled polymer composites,^{35,36} a knee or discontinuity has been observed at a stress corresponding to 23 MPa ($\epsilon = 0.35\%$),³² independent of filler concentration. This threshold stress corresponds to an onset of stress whitening due to crazing and only occurs when the beads are untreated (i.e., no coupling agent). These untreated beads have poor adhesion with the PPO matrix and being unable to support the tensile load act as stress concentrators. As evident from the stress-strain curves for the PpClS/PPO blends (Fig. 4), no such discontinuity is observed for the polymer blends. This further supports the evidence from the behavior of the break strength of these blends that there is strong interfacial adhesion between phases in the incompatible blends.

V. CONCLUSIONS

(1) Both compatible and semicompatible PPO blends that show blend densification exhibit a small synergistic maximum in their modulus-composition plots which can be modeled by the classical rule of mixtures for composites with an additional interaction term. The incompatible PPO blends exhibit no blend densification and can be modeled adequately by the series model for composites.

(2) In terms of the relative magnitude of the size of the effect, tensile stress and elongation at break (or yield) are more sensitive than modulus to changes in the compatibility of the blend. The compatible PPO blends exhibit a maximum in strength at high PPO blend compositions. The semicompatible (transitional) and incompatible blends exhibit both a minimum in the blend composition range in which brittle fracture predominates and an apparent maximum in the ductile zone. Qualitative application of the Nielsen model for break strength of composites suggests that the mini-

imum in break strength occurring at about 15% PPO in the semicompatible PPO blends is indicative of strong interfacial adhesion between phases.

(3) Although some insight into the mechanical properties of incompatible polymer blends can be gleaned from an understanding of the way polymer composites with rigid fillers behave, the full picture is more complex. Factors that influence mechanical properties such as the shape, size, degree of agglomeration, and interfacial adhesion of the dispersed phase³⁷ intimately depend upon particular processing conditions and the degree of miscibility of components in the blend. An additional complication in the particular case of incompatible polymer blends is the occurrence of phase inversion and the possibility of two continuous phases. Additional controlled studies may suggest ways that immiscible polymers may be blended to achieve attractive mechanical properties.

¹D.R. Paul, C.E. Vinson, and C.E. Locke, *Polym. Eng. Sci.* **12**, 157 (1972).

²(a) L.W. Kleiner, F.E. Karasz, and W.J. MacKnight, SPE 36th Annual Technical Conference, Washington, D.C., 1978, pp. 243-248 (unpublished); *Polym. Eng. Sci.* **19**, 519 (1979); (b) L.W. Kleiner, Ph.D. dissertation, University of Massachusetts, 1978.

³A.F. Yee, *Polym. Prepr., Am. Chem. Soc. Div. Polym. Chem.* **17**, 145 (1976); *Polym. Eng. Sci.* **17**, 213 (1977).

⁴S. Wellinghoff and E. Baer, *Am. Chem. Soc. Div. Org. Coatings Plast. Chem. Pap.* **36**, 140 (1976); *J. Appl. Polym. Sci.* **22**, 2025 (1978).

⁵W.J. MacKnight, F.E. Karasz, and J.R. Fried, in *Polymer Blends*, edited by D.R. Paul and S. Newman (Academic, New York, 1978), Vol. I., pp. 185-242.

⁶J.R. Fried, F.E. Karasz, and W.J. MacKnight, *Macromolecules* **11**, 150 (1978).

⁷(a) F.E. Karasz, W.J. MacKnight, and J.J. Tkacik, *Polym. Prepr. Am. Chem. Soc. Div. Polym. Chem.* **15**, 415 (1974); (b) J.J. Tkacik, Ph.D. dissertation, University of Massachusetts, 1976.

⁸A.R. Shultz and B.M. Beach, *Macromolecules* **7**, 902 (1974).

⁹P.R. Couchman, *Macromolecules* **11**, 1156 (1978).

¹⁰R.E. Wetton, W.J. MacKnight, J.R. Fried, and F.E. Karasz, *Macromolecules* **11**, 158 (1978).

¹¹J. Letz, *J. Polym. Sci. Polym. Phys. Ed.* **7**, 1987 (1969).

¹²B. Maxwell, *SPE J.* **28**, 24 (1972).

¹³J.R. Fried, Ph.D. dissertation, University of Massachusetts, 1976.

¹⁴W.J. Jackson, Jr., and J.R. Caldwell, *J. Appl. Polym. Sci.* **11**, 227 (1967).

¹⁵N. Sundgren, G. Bergman, and Y.J. Shur, *J. Appl. Polym. Sci.* **22**, 1255 (1978).

¹⁶G. Bergman, H. Bertilsson, and Y.J. Shur, *J. Appl. Polym. Sci.* **21**, 2953 (1977).

¹⁷E.P. Cizek, U.S. Patent 3,383,435 (assigned to General Electric), August 11, 1967.

¹⁸L.E. Nielsen, *Mechanical Properties of Polymers and Composites* (Marcel Dekker, New York, 1974), p. 397.

¹⁹Reference 18, p. 401.

²⁰L.J. Cohen and O. Ishai, *J. Compos. Mater.* **1**, 390 (1967).

²¹L.E. Nielsen, *Predicting the Properties of Mixtures: Mixture Rules in Science and Engineering* (Marcel Dekker, New York, 1978), p. 22.

²²S.T. Wellinghoff, J.L. Koenig, and E. Baer, *J. Polym. Sci. Polym. Phys. Ed.* **15**, 1913 (1977).

²³K.L. Trachte and A.T. DiBenedetto, *Int. J. Polym. Mater.* **1**, 75 (1971).

²⁴A. Wambach, K. Trachte, and A. DiBenedetto, *J. Compos. Mater.* **2**, 266 (1968).

²⁵H. Van Oene, in *Polymer Blends*, edited by D.R. Paul and S. Newman (Academic, New York, 1978), Vol. I, pp. 295-352.

²⁶L. Nicolais and A.T. DiBenedetto, *J. Appl. Polym. Sci.* **15**, 1585 (1971).

²⁷F. Bueche, *Physical Properties of Polymers* (Wiley-Interscience, New York, 1962), p. 202.

²⁸L.R. Schmidt, *J. Appl. Polym. Sci.* **23**, 2463 (1979).

²⁹R. Buchdahl, *J. Polym. Sci.* **28**, 239 (1958).

³⁰M. Schrager, *J. Appl. Polym. Sci.* **22**, 2379 (1978).

³¹L.E. Nielsen, *J. Appl. Polym. Sci.* **10**, 97 (1966).

³²R.E. Lavengood, L. Nicolais, and M. Narkis, *J. Appl. Polym. Sci.* **17**, 1173 (1973).

³³A.S. Kenyon and H.J. Duffy, *Polym. Eng. Sci.* **7**, 189 (1967).

³⁴M.R. Piggot and J. Leidner, *J. Appl. Polym. Sci.* **18**, 1619 (1974).

³⁵L. Nicolais and M. Narkis, *Polym. Eng. Sci.* **11**, 194 (1971).

³⁶L. Nicolais, E. Drioli, and R.F. Landel, *Polymer* **14**, 21 (1973).

³⁷G.W. Brasell and K.B. Wischmann, SPE Regional Technical Conference on Advances in Reinforced Thermoplastics, El Segundo, Calif., 1972, Paper 1, pp. 1-16 (unpublished).